Long-distance correlations in TCABR biasing experiments

2012 Nucl. Fusion 52 063004

(http://iopscience.iop.org/0029-5515/52/6/063004)

Nucl. Fusion **52** (2012) 063004 (8pp) doi:10.1088/0029-5515/52/6/063004

Long-distance correlations in TCABR biasing experiments

Yu.K. Kuznetsov[1], I.C. Nascimento[1], C. Silva[2], H. Figueiredo[2], Z.O. Guimarães-Filho[1,3], I.L. Caldas[1], R.M.O. Galvão[1,4], J.H.F. Severo[1], D.L. Toufen[1], L.F. Ruchko[1], A.G. Elfimov[1], J.I. Elizondo[1], W.P. de Sá[1], O.C. Usuriaga[1], E. Sanada[1], A.V. Melnikov[5], M.P. Gryaznevich[6], M. Peres Alonso[2], A.P. Reis[1], M. Machida[7], D.J. Trembach[8], T.M. Germano[1], R. Narayanan[9], M. Ghoranneviss[10], R. Arvin[10], S. Mohammadi[10], S.R.S. Tekieh[10], F.O. Borges[1], V. Bellintani[11], G.P. Canal[2], P. Duarte[7], R.M. de Castro[9], G. Vorobyov[12], M. Mizintseva[12], V.E. Moiseenko[13], F. do Nascimento[9], G. Ronchi[7] and L.M.F. Schmutzler[7]

[1] Institute of Physics, University of São Paulo, São Paulo, Brazil
[2] Associação Euratom/IST, Instituto de Plasma e Fusão Nuclear, Instituto Superior Técnico, Lisboa, Portugal
[3] Aix-Marseille Univ., CNRS PIIM UMR 7345, International Institute for Fusion Science, Marseille, France
[4] Brazilian Center for Research in Physics, Rio de Janeiro, Brazil
[5] Institute of Nuclear Fusion, RRC 'Kurchatov Institute', Moscow, Russia
[6] EURATOM/UKAEA Fusion Association, Culham SC, Abingdon, UK
[7] Institute of Physics, University of Campinas, Campinas, Brazil
[8] Plasma Physics Laboratory, University of Saskatchewan, Saskatoon, Canada
[9] Plasma Associate Laboratory, National Institute for Space Research, São Jose dos Campos, Brazil
[10] Plasma Physics Research Center, Islamic Azad University, Tehran, Iran
[11] Faculty of Technology of São Paulo, São Paulo, Brazil
[12] Faculty of Applied Mathematics and Control Processes, Saint-Petersburg State University, Saint-Petersburg, Russia
[13] NSC 'Kharkov Institute of Physics and Technology', Kharkov, Ukraine

E-mail: yuk@if.usp.br

Received 6 July 2011, accepted for publication 20 March 2012
Published 17 April 2012
Online at stacks.iop.org/NF/52/063004

Abstract
Long-distance correlations (LDCs) of plasma potential fluctuations in the plasma edge have been investigated in the TCABR tokamak in the regime of edge biasing H-mode using an array of multi-pin Langmuir probes. This activity was carried out as part of the scientific programme of the 4th IAEA Joint Experiment (2009). The experimental data confirm the effect of amplification of LDCs in potential fluctuations during biasing recently observed in stellarators and tokamaks. For long toroidal distances between probes, the cross-spectrum is concentrated at low frequencies $f < 60$ kHz with peaks at $f < 5$ kHz, $f = 13$–15 kHz and $f \sim 40$ kHz and low wave numbers with a maximum at $k = 0$. The effects of MHD activity on the LDCs in potential fluctuation are investigated.

(Some figures may appear in colour only in the online journal)

1. Introduction

Turbulence-driven zonal flows (ZFs) together with mean $E \times B$ sheared flows generated by various other mechanisms are considered as one of the important phenomena for understanding the transition from low to high (L–H) confinement regimes. As predicted by theory and observed in many experiments [1, 2], ZFs occur in tokamaks and stellarators as symmetric ($n = m = 0$) electrostatic potential fluctuations with a finite radial wavenumber. Therefore, the experimental study of long-distance correlations (LDCs), which are naturally expected in this case, is an important

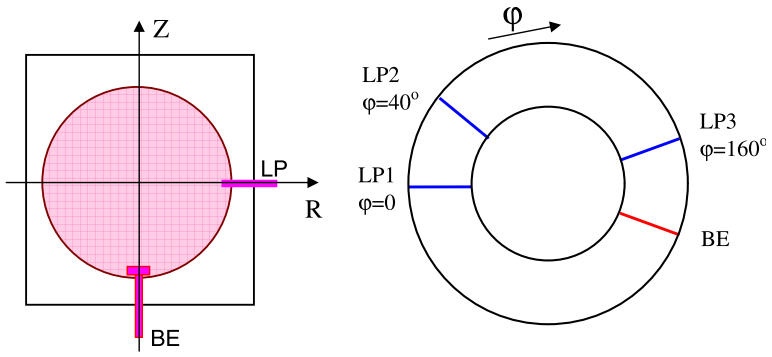

Figure 1. Biasing electrode (BE) and Langmuir probe (LP1, LP2, LP3) positions in poloidal (left part) and toroidal (right part) directions.

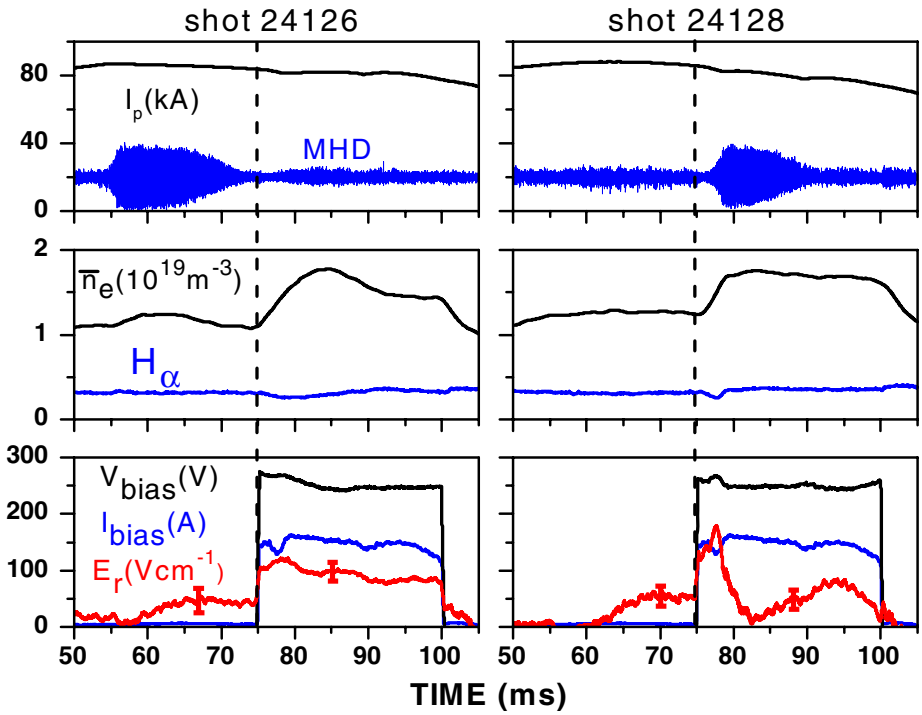

Figure 2. Time evolution of plasma parameters with electrode biasing ($t = 75$–100 ms) for two discharges with bursts of high MHD activity before biasing (shot 24126) and during biasing (shot 24128). (Top panels) plasma current I_p and MHD activity; (middle panels) line-averaged plasma density $\bar{n}_e$ and H_α emission; (bottom panels) electrode voltage and current V_{bias}, I_{bias} and average radial electric field E_r at $r/a = 0.94$–0.97 together with root mean square level of fluctuations.

issue. Recent results obtained in experiments with a biasing electrode carried out on the TJ-II stellarator and on the ISTTOK and TEXTOR tokamaks indicate amplification of LDCs in potential fluctuations during transition to the H-regime, while the density fluctuations show low correlation [3–5]. Similar experiments carried out on the TJ-K stellarator have observed LDCs also in density fluctuations [6]. These highly correlated potential fluctuations have vanishing poloidal and toroidal wave numbers, $m \sim n \sim 0$. An increase in the LDCs has also been observed in the TJ-II stellarator during a spontaneous L–H bifurcation in experiments with an NBI-heated plasma [7].

In this paper we present results obtained in experiments carried out on the TCABR tokamak ($a = 0.18$ m, $R_0 = 0.615$ m, $B_t = 1.1$ T) to investigate the effect of amplification of LDCs with external electrostatic biasing as part of an experimental campaign organized within the framework of the IAEA Coordinated Research Project on 'Joint Experiments Using Small Tokamaks' (May 2009).

2. Experimental setup

The external electrostatic biasing was applied by a graphite electrode of 8 mm height and 20 mm diameter, inserted vertically 15 mm into the edge plasma, at the bottom of the plasma column. The floating potential was measured at the plasma edge with three multi-pin Langmuir probe arrays located at different toroidal positions: a 6-pin forked probe (LP1), a 5-pin probe (LP2), and a 20-pin rake probe (LP3). The locations of the electrode and Langmuir probes are shown in figure 1. The signals of the probes were acquired with a 2 MHz sampling rate.

The time evolution of the main plasma parameters is presented in figure 2 for two typical discharges with electrode

biasing. In these experiments, the plasma current was kept within the range $I_p = 80$–85 kA and the line-averaged electron density was adjusted at $\bar{n} \approx (1.0$–$1.2) \times 10^{19}\,\mathrm{m}^{-3}$. The plasma density increases during biasing without increasing H_α emission indicating improved particle confinement.

The level of magnetic fluctuations detected by a poloidal set of 22 Mirnov probes near the plasma boundary, $r = 19.5$ cm, is rather high in our experiments. Bursts of the resistive tearing mode 2/1 are frequently triggered. At the radial position of the probes, the amplitude of the background magnetic fluctuations is about $\tilde{B}/B_p \sim 1.5 \times 10^{-3}$ increasing to $\sim 10^{-2}$ during the bursts of high MHD activity; here B_p is the poloidal component of the equilibrium magnetic field. The magnetic island $m/n = 3/1$ is also generated due to the toroidal mode coupling, causing strong modulation of the potential at the plasma edge, $r = 16$–18 cm.

The two regimes shown in figure 2 were chosen for the analysis as reproducible and favourable for studies of the effect of high MHD activity on LDCs in ohmic and bias regimes.

As in discharge 24126, the MHD burst appeared in many discharges in the time interval 55–70 ms in the usual ohmic regime and biasing was applied after the burst. In this regime, the MHD triggers a small increase in plasma density without visible changes in other main plasma parameters and H_α emission.

In the other regime, exemplified by discharge 24128, the MHD burst was triggered by biasing. This regime was most reproducible in our experiments with electrode biasing. In this case, the MHD activity has a strong negative effect on the edge transport barrier, as has already been observed in previous experiments with a biased electrode on TCABR [8, 9]. The reason is that the magnetic island 3/1 at the plasma edge is large enough to decrease the radial electric field produced by biasing and thus deteriorate the transport barrier. One can see that the average radial electric field measured at the plasma edge with two probes separated radially by 0.5 cm ($r/a = 0.94$–0.97) drops to almost zero level with the MHD burst and then recuperates slowly, while the level of MHD activity is still high (similar behaviour of the mean E_r during biasing was observed in previous experiments [8, 9]).

The probability of occurrence of MHD bursts increases with biasing. To keep the MHD activity somewhat under control and avoid disruptions, the electrode voltage was kept at a value lower than that in [8, 9], providing a moderate increase in plasma density with biasing, from 1.0–1.2 up to $(1.6$–$1.8) \times 10^{19}\,\mathrm{m}^{-3}$.

3. Cross-correlation of potential fluctuations at the plasma edge

Typical raw signals of the floating potential are presented in figure 3. They show significant time variation of the mean value (trend) with nearly constant electrode voltage ~250 V and current ~150 A. In general, the trend results in an artificial increase in the calculated amplitudes of the oscillations at low frequencies [10], being particularly important at frequencies below 1 kHz in our case (figure 4). Therefore, it was removed from raw signals in the analysis of turbulent fluctuations. The mean values of V_f measured by distant probes are strongly correlated at the same radial position (signals a, b and c), and

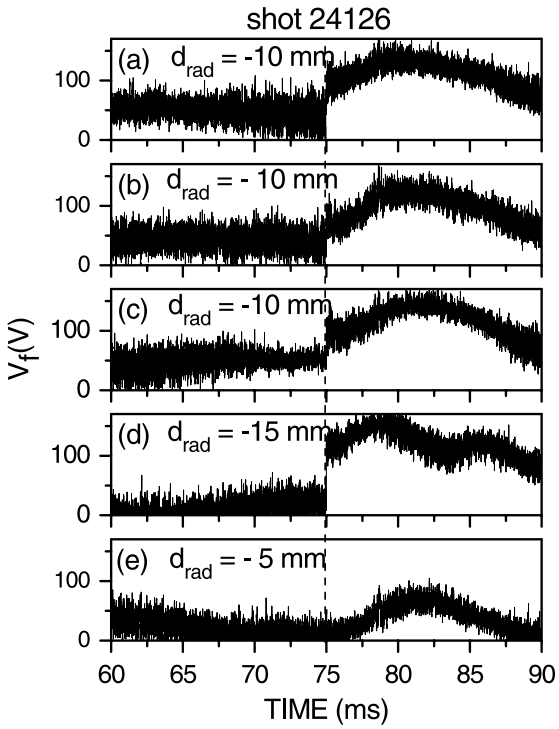

Figure 3. Time evolution of floating potential for different probes (shot 24126, $t = 60$–90 ms). (a) Probe array LP1, radial distance from the limiter to the probe $d_{rad} = r - a = -10$ mm; (b) LP2, $d_{rad} = -10$ mm; (c) LP3, $d_{rad} = -10$ mm; (d) $d_{rad} = -15$ mm; (e) $d_{rad} = -5$ mm.

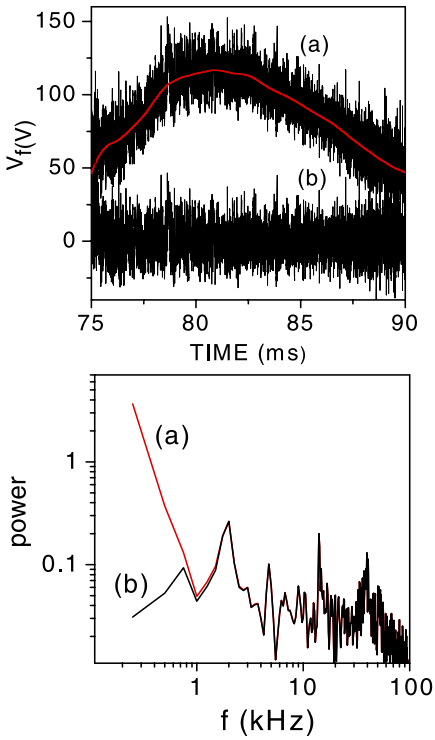

Figure 4. Effect of time evolution of the potential mean value (trend) on the power spectrum of potential fluctuations. Top panel: (a) floating potential V_f and its calculated mean value $V_{f,mean}$ and (b) fluctuations of the potential without trend $\tilde{V}_f = V_f - V_{f,mean}$. Bottom panel: ($a$) spectrum of V_f and (b) spectrum of $\tilde{V}_f$.

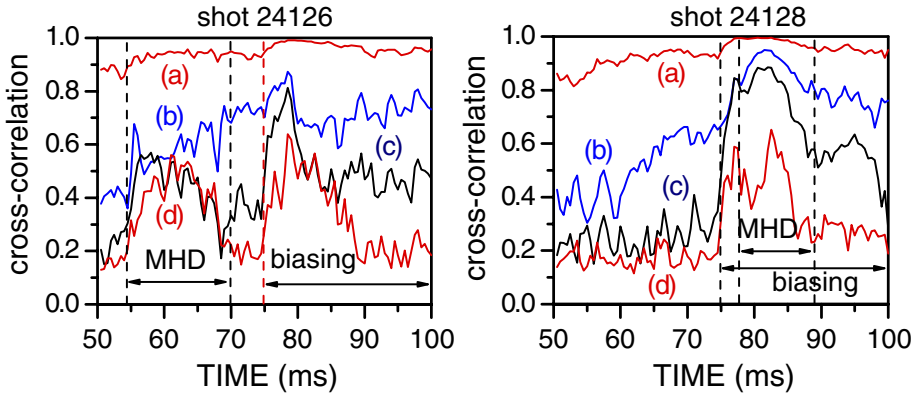

Figure 5. Time evolution of cross-correlation for the two discharges of figure 2 and different distances between probes. (*a*) Poloidal distance $d_{\rm pol} = 0{,}4$ cm, $r/a = 0.97$ (array LP1 in figure 1); (*b*) radial distance $d_{\rm rad} = 0.5$ cm, $r/a = 0.94$–0.97 (LP1); (*c*) toroidal distance $d_{\rm tor} = 55$ cm, $\Delta\varphi = 40^\circ$, $r/a = 0.94$ (LP1–LP2); (*d*) toroidal distance $d_{\rm tor} = 219$ cm, $\Delta\varphi = 160^\circ$, $r/a = 0.94$ (LP1–LP3).

they are rather sensitive to the radial position (signals *d* and *e*). The similar shape of the mean value can be used as the evidence of close radial positions of distant probes.

The cross-correlation between two signals (x, y) is defined as

$$C_{xy} = \langle[x(t+\tau)-\bar{x}][y(t)-\bar{y}]\rangle/\sqrt{\langle[x(t)-\bar{x}]^2\rangle\langle[y(t)-\bar{y}]^2\rangle^2},$$

where τ is the time lag. The maximum absolute value of the function C_{xy} (τ) was calculated, and its time evolution is presented in figure 5, for both regimes shown in figure 2 and various distances between probes.

Let us first consider the behaviour of cross-correlation in the case of short separations between probes. The case of 0.4 cm poloidal distance is indicated by curves (a); curves (b) correspond to probes separated radially by 0.5 cm (LP1). The correlation length L can be estimated assuming exponential decay of cross-correlation with distance $C_{xy} = \exp(-d/L)$. In the ohmic phase with low MHD activity (shot 24128), we obtain $L_{\rm pol} = 2$–4 cm and $L_{\rm rad} = 0.5$–1 cm. Both poloidal and radial correlation lengths show significant time variations and the observed values are in agreement with data from many previous experiments in tokamaks and stellarators [11]. In the biasing phase with low MHD activity (shot 24126), the correlation length increases strongly, $L_{\rm pol} = 8$–40 cm and $L_{\rm rad} = 2$–3 cm, with maximum values reached just after the application of the bias voltage. Thus, the effect of amplification of poloidal and radial correlation in the L–H transition can already be concluded from the short-distance measurements. More detailed information requires larger separation between probes.

Array LP1 (forked probe) allows measurements with 3 cm poloidal distance. In the ohmic phase, we obtain $C_{xy} = 0.3$–0.5 and $L_{\rm pol} = 2.5$–4 cm and in the biasing phase $C_{xy} = 0.60$–0.86 and $L_{\rm pol} = 6$–20 cm.

The toroidal LDCs are revealed in the other two curves, (c) and (d) of figure 5. Here the same probe of the LP1 array ($\varphi = 0$ in figure 1) was chosen as the reference one and the second probe was chosen in LP2 (c) and LP3 (d) arrays. The corresponding distances between probes in the toroidal direction along the magnetic surface are 55 cm ($\Delta\varphi = 40^\circ$) and 219 cm ($\Delta\varphi = 160^\circ$). One can see amplification of the cross-correlation, up to 0.5–0.8, due to biasing and MHD instability. In the case of a mild toroidal distance 55 cm (curve (c)) without biasing and with low MHD (shot 24128, ohmic phase), the cross-correlation is low $C_{xy} = 0.1$–0.2 (taking into account the noise level ~0.1) and $L_{\rm tor} \sim 30$ cm. With biasing (shot 24126), the maximum cross-correlation is $C_{xy} = 0.8$ and $L_{\rm tor} \sim 240$ cm. In the case of toroidal distance 219 cm, which is close to the maximum possible toroidal distance between probes ($\varphi = \pi$), high cross-correlation is observed in the biasing phase $C_{xy} = 0.6$ and $L_{\rm tor} \sim 430$ cm (shot 24126, curve (d)).

We would like to note that in the improved confinement regime the correlation reaches its maximum value just after the application of the bias and then decays with a time constant of 5–10 ms, as has already been observed on TJ-II during the spontaneous L–H transition [7].

As was expected, the burst of coherent high-level MHD instability also results in LDCs in both ohmic and biasing regimes. This is just an effect of the magnetic island 3/1 at the plasma edge associated with the MHD activity. This effect is highly pronounced in the ohmic phase for a toroidal distance of 219 cm (shot 24126, curve (d)), when the cross-correlation without MHD is low (shot 24128, curve (d)).

The effect of both biasing and strong MHD oscillations (shot 24128, $t = 75$–100 ms) on LDCs and plasma confinement is rather involved. This is more clearly shown for curve (d): the correlation rises to $C_{xy} = 0.6$ during the first 3 ms of the biasing phase similar to shot 24126, reduces sharply to $C_{xy} = 0.4$ as the MHD activity sets in, and then increases again. This behaviour of LDCs is similar to the behaviour of the radial electric field shown in figure 2.

The effect of MHD burst on the plasma confinement in the bias phase is very different from that observed in the ohmic phase. Usually, a small increase in the plasma density during the MHD burst is observed in the ohmic discharges without a visible change in the H_α emission and plasma current (figure 2). Therefore, one may speculate on a small improvement in the plasma confinement due to the MHD activity. As is known, a possible mechanism to explain this may be a mild internal transport barrier formation in the vicinity of the magnetic island 2/1, in spite of this instability being usually associated with deterioration of plasma confinement. In any case, even if this improvement exists, it is rather weak in our case. In contrast,

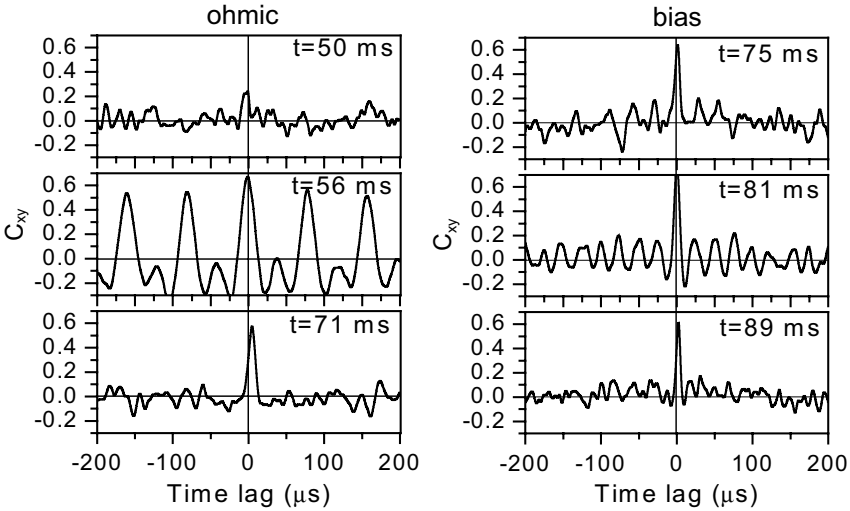

Figure 6. Cross-correlation function of potential fluctuations at different times before (left panels) and during (right panels) biasing for poloidal distance $d_{\mathrm{pol}} = 3$ cm (LP1); discharge 24126.

the effect of MHD burst on the plasma confinement in the biasing phase is always strong and negative, most probably due to the destruction of the edge transport barrier by the island 3/1, as was discussed in previous studies on electrode biasing in TCABR [8, 9]. The negative effect of MHD burst on the plasma confinement was also observed in the TUMAN-3M tokamak in the ohmic H-mode regime [12, 13].

Examples of $C_{xy}\,(t, \tau)$ for different times t are shown in figure 6 for a poloidal separation of 3 cm between probes. The periodic peaks shown in the cross-correlation at $t = 56$ ms (ohmic phase) correspond to regular oscillations at the MHD frequency (13 kHz) and its second harmonic, which occur during high MHD activity. This coupling between drift-type electrostatic turbulence and magnetic MHD fluctuations has already been observed in TCABR [14] and other tokamaks [15, 16]. In all other cases, the wide spectrum is mostly responsible for the correlation as one can conclude from the relatively narrow peaks of $C_{xy}\,(\tau)$ near $\tau = 0$.

The coherence, defined as the normalized cross-power spectrum $\gamma_{xy} = |S_{xy}(f)|/\sqrt{S_x(f)S_y(f)}$, where S_{xy} is the cross-power spectrum and S_x and S_y are the autopower spectra, is presented in figure 7 for various distances between probes.

The calculations were performed for time intervals 55–75 ms (ohmic phase) and 75–90 ms (bias phase) with 1 ms time window and 2 MHz sampling rate. For a small poloidal distance 0.4 cm, the coherence increases with biasing for all frequencies up to the maximum measured frequency of 300 kHz. With the increase in the separation between probes, the coherence decreases for higher frequencies. In the case of the longest toroidal distance of 219 cm, the coherence is significant for frequencies below 60 kHz. It shows pronounced peaks at frequencies $f < 5$ kHz, $f = 14$–15 kHz and $f \sim 40$ kHz. In the ohmic phase, only peaks of coherence due to the MHD activity are observed at the main frequency $f = 13$ kHz and its second and third harmonics in the case of long distances.

An important information about the spatial structure of potential fluctuations can be obtained from the wavenumber–frequency power spectrum $S(k, f)$ estimated using the digital

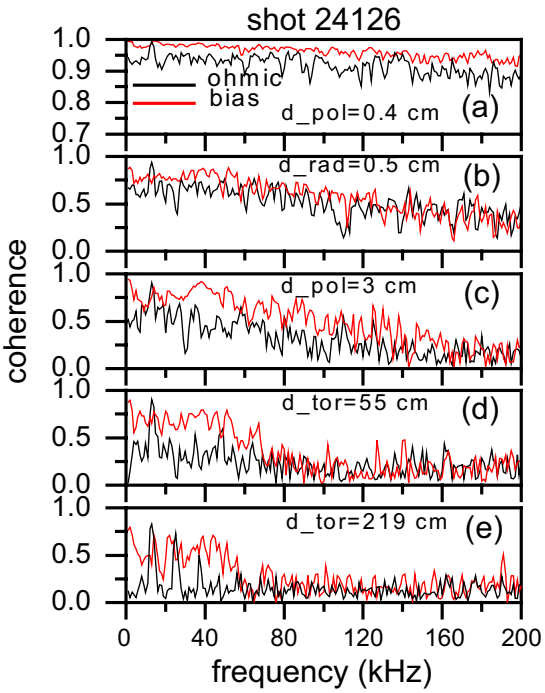

Figure 7. Coherence of potential fluctuations for ohmic (black lines) and biasing (red lines) phases of shot 24126 and different distances between probes. (*a*) Poloidal distance $d_{\mathrm{pol}} = 0.4$ cm, (*b*) radial distance $d_{\mathrm{rad}} = 0.5$ cm, (*c*) poloidal distance $d_{\mathrm{pol}} = 3$ cm, (*d*) toroidal distance $d_{\mathrm{tor}} = 55$ cm, (*e*) toroidal distance $d_{\mathrm{tor}} = 219$ cm. Radial position (*a*) $r/a = 0.97$; (*b*) $r/a = 0.97$–0.94; (*c*)–(*e*) $r/a = 0.94$.

method introduced by Beall, Kim and Powers for the analysis of probe pairs' data [17, 18]. In this method, the statistical $S(k, f)$ is calculated from the fluctuations measured at two fixed spatial points and it is based on the consideration that under the condition of fully developed turbulence the frequency and the wavenumber are stochastically related. It must be noted that the $S(k, f)$ estimated by the two-point technique may not correspond to the true $S(k, f)$ when more than one dominant

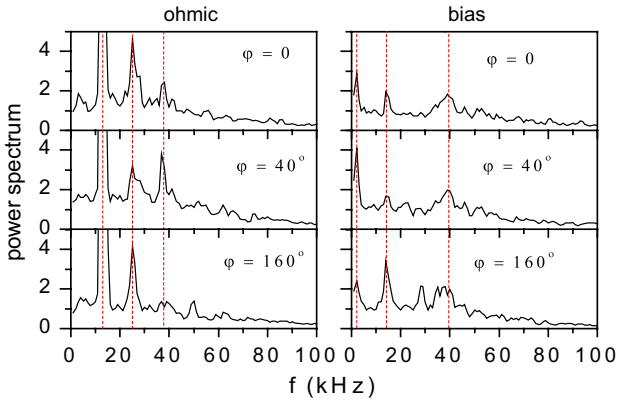

Figure 8. Frequency spectra of potential fluctuations in the ohmic (left) and bias (right) phases of shot 24126 at different toroidal positions $\varphi = 0$, 40° and 160° and the same radial position $r/a = 0.94$. Reproducible peaks are indicated by vertical dashed lines: $f = 13$ kHz and its second and third harmonics in the ohmic phase; $f < 5$ kHz, $f = 14$–15 kHz and $f \sim 40$ kHz in the biasing phase. In the ohmic phase, amplitudes of main peaks at $f = 13$ kHz are $S_{13} = 17$ au ($\varphi = 0$), 28 au ($\varphi = 40°$) and 35 au ($\varphi = 160°$).

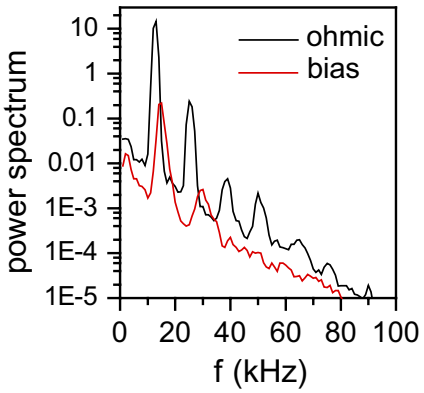

Figure 9. Spectra of magnetic oscillations measured by Mirnov probes near the plasma boundary ($r = 19.5$ cm) in ohmic (black line) and bias (red line) phases of shot 24126. The observed peaks correspond exactly to the ones shown in the spectra of potential fluctuations.

mode exists at a given frequency [19]. The frequency and wavenumber power spectra $S(f)$ and $S(k)$ are calculated by adding $S(k, f)$ on k and f, respectively.

The autopower spectra $S(f)$ for different probe positions are presented in figure 8 for shot 24126. In the ohmic phase the main peak corresponds to the MHD frequency $f = 13$ kHz and smaller peaks to its second and third harmonics. In the biasing phase, peaks $f < 5$ kHz, $f = 14$–15 kHz, and the rather smooth maximum at the $f \sim 40$ kHz are observed reproducibly. The resonance $f = 14$–15 kHz in the biasing phase is strongly correlated with low-level oscillations of the poloidal magnetic field measured by Mirnov probes (figure 9). We believe that the low-frequency mode, $f <$ 5 kHz, corresponds to ZFs. The oscillatory one at $f \sim 40$ kHz has the poloidal mode structure expected for geodesic acoustic modes (GAMs), although its frequency is much larger than the theoretical value for the parameters at the plasma edge ($f \sim$ 15–20 kHz). Nevertheless, we point out that a broad range of values for the frequency of GAMs has been reported in the literature [2].

Let us discuss the experimental data on the effect of MHD instability on potential fluctuations at the plasma edge in more detail. Strong modulation of the floating plasma potential and other plasma parameters by the MHD activity (saturated magnetic islands) was observed in TCABR in previous experiments [8, 9]. In the present experiment, we operate in a regime with a dominant $m/n = 2/1$ mode with a satellite $m/n = 3/1$ mode; the corresponding magnetic island 3/1 is located at $r = 16.5$–17 cm. The instability appears as a burst of quasi-sinusoidal highly coherent oscillations, $\gamma_{12} > 0.99$, both in the poloidal and toroidal directions. The electrostatic potential fluctuations at the plasma edge have the same main frequency of the MHD oscillations and smaller but rather high coherence: $f = 13$ kHz, $\gamma_{12} = 0.8$–0.9 for high MHD activity during the ohmic regime (shot 24126). The coherence increases even further when MHD increases during the biasing regime, $f = 11$ kHz, $\gamma_{12} = 0.95$ (shot 24128), for a maximum toroidal distance of 219 cm.

We observe a rather large spread of data on the mode number obtained for different combinations of probes and a strong decrease in the estimated value of the mode number with biasing. The calculated statistical $S(k, f)$ and $S(k)$ spectra for small poloidal distance 0.4 cm show that in the biasing phase the turbulent broadening in wavenumber domain decreases strongly with a pronounced maximum at $k = 0$ (figure 10). In the ohmic phase with MHD, the wavenumber spectrum has two maxima of $S(k)$: a sharp peak at $k_\vartheta \approx -0.4\,\mathrm{cm}^{-1}$ and a broad one at $k_\theta \approx 0.5\,\mathrm{cm}^{-1}$. The estimated poloidal mode number for the first maximum, $m = r_\mathrm{p} k_\theta$, where $r_\mathrm{p} = 17.5$ cm is the radial probe position, is about $m = 7$, i.e. significantly different from the value of $m = 3$ associated with the more external island. Therefore, in spite of the electrostatic and magnetic perturbations being frequency-locked, they have quite different poloidal structures. The data on poloidal and toroidal mode numbers obtained for shots 24126 and different combinations of probes show rather large spread: $m = 2$–7, $n = 0.2$–1.6 for the ohmic regime and $m = 0$–1.5, $n = 0$–0.6 for the bias regime. This indicates that while the poloidal mode structure of the electrostatic fluctuations is of the type expected for standard drift waves in the ohmic regime, it comes close to that expected for ZFs in the bias regime. The toroidal mode number is estimated as $n = k_\varphi R_\mathrm{p}$. Here $R_\mathrm{p} = R_0 + r_\mathrm{p}$ is the radial co-ordinate of the probes located at the low magnetic field side ($Z = 0$) of the torus, as shown in figure 1, and r_p is the minor radius of the magnetic surface, $r_\mathrm{p} = 17$ cm, $R_0 = 61.5$ cm. The data for the low (shot 24126, figure 10(*b*)) and high (shot 24128, not shown here) MHD activity are similar at this point, i.e. the estimated mode numbers of potential fluctuations with MHD frequency have low values in the bias regime.

One can see in figure 10 that the peaks at $f < 5$ kHz and $f \sim 40$ kHz, already shown in figure 8, appear in the statistical $S(k, f)$ plot also with low values of wavenumber close to $k_\theta = 0$. The $S(k, f)$ and $S(k)$ spectra for the long poloidal distance 3 cm and toroidal distance 219 cm are presented in figures 11 and 12. The wavenumber is calculated from the cross-phase $\theta_{xy}(f)$ as $k(f) = \theta_{xy}(f)/d$, where d is the distance between probes. The condition $-\pi < \theta_{xy} < \pi$ has to be fulfilled to avoid the 2π phase ambiguity, i.e. for a given distance d, the value of wavenumber is limited as $|k(f)| < |k|_\mathrm{max}$, where $|k_\mathrm{max}| = \pi/d$. For the poloidal distance 0.4 cm, we have

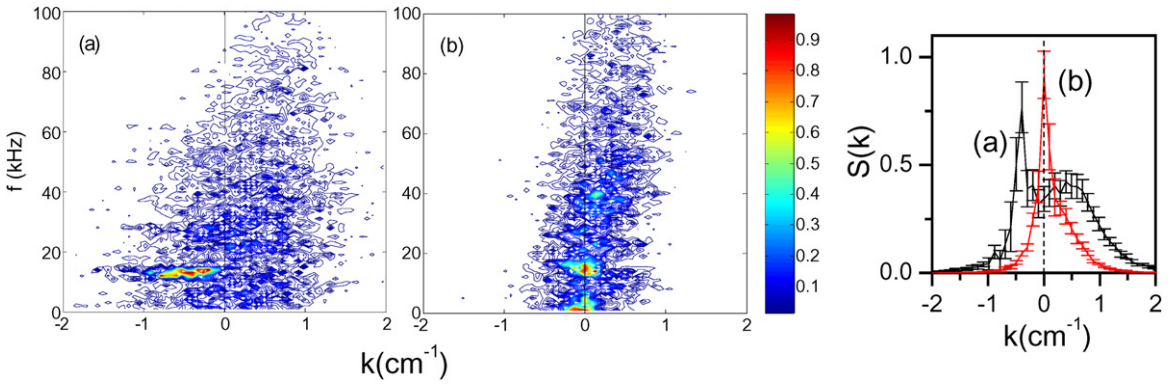

Figure 10. Wavenumber–frequency spectra $S(k, f)$ and wavenumber spectra $S(k)$ of potential fluctuations for poloidal distance 0.4 cm and radial position $r/a = 0.97$; (a) ohmic phase and (b) biasing phase, shot 24126.

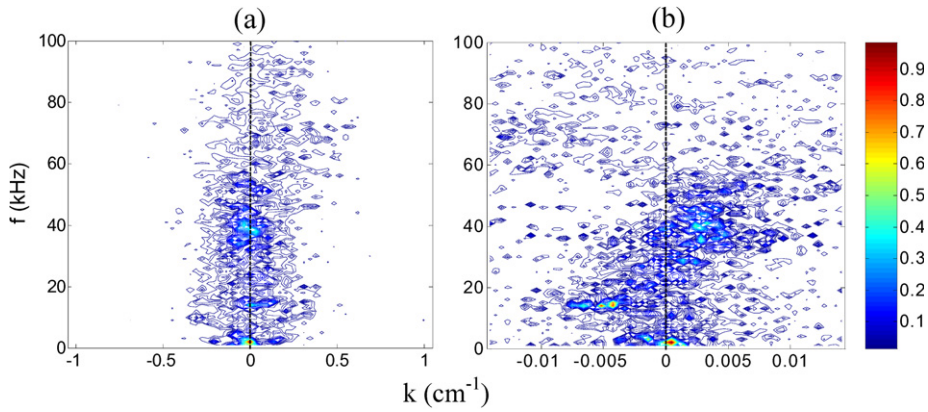

Figure 11. Wavenumber–frequency spectra $|S_{xy}(k, f)|$ of potential fluctuations for the biasing phase of shot 24126. (a) Poloidal distance 3 cm; (b) toroidal distance 219 cm; radial position $r/a = 0.94$.

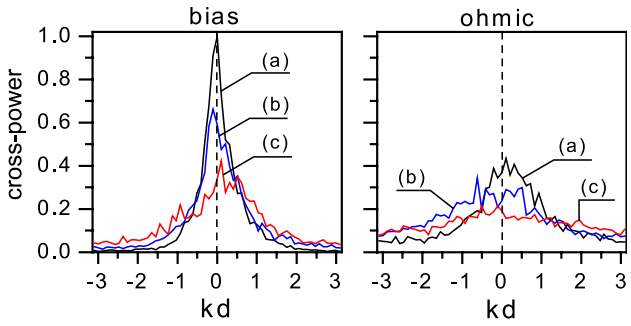

Figure 12. Cross-power spectra of potential fluctuations as a function of the cross-phase $\theta_{xy} = kd$ for different distances $d$between probes: (a) poloidal distance 3 cm; (b) toroidal distance 55 cm; (c) toroidal distance 219 cm; (left part) biasing phase of shot 24126 and (right part) ohmic phase of shot 24128, both with low MHD activity.

$|k_{\max}| \approx 7.8\,\mathrm{cm}^{-1}$, and the maximum measured wave numbers are substantially lower than this value both in the ohmic and biasing regimes (figure 10). For this small distance, the power spectra have close values, $S_x(f) \cong S_y(f) \cong |S_{xy}(f)|$, due to the high correlation of potential fluctuations (figures 5 and 7); hence one can use any of these functions in the plots of $S(k, f)$ and $S(k)$ in figure 10. For distances of 3 cm in the poloidal direction, 55 cm in the toroidal direction and especially 219 cm in the toroidal direction, both these conditions are not valid. In this case, it is reasonable to plot the wavenumber–frequency spectra $|S_{xy}(k, f)|$ providing information on the correlated fluctuations. The cross-power spectra in the space domain $S_{xy}(k)$ calculated for regimes of low MHD activity, i.e. for the biasing phase of shot 24126 and the ohmic phase of shot 24128, show that the condition $|\theta_{xy}| < \pi$ is reasonably fulfilled (S_{xy} is rather small at $\theta_{xy} = \pm\pi$) in the biasing phase, even for the maximum toroidal distance of 219 cm. Compared with the ohmic phase, biasing results in strong increase and concentration of cross-power near $\theta_{xy} = 0$ (figures 11 and 12)

The wavenumber–frequency spectra $|S_{xy}(k, f)|$ in the biasing phase of shot 24126 for the poloidal distance of 3 cm, $|k_{\theta,\max}| \approx 1\,\mathrm{cm}^{-1}$, and toroidal distance of 219 cm, $|k_{\varphi,\max}| \approx 0.014\,\mathrm{cm}^{-1}$, are presented in figure 11. The spectra show peaks of amplitude in the frequency and wavenumber domains, $k_\theta \sim 0$ for $f < 5$ kHz, $k_\varphi \approx -0.004\,\mathrm{cm}^{-1}$ for $f = 14$–15 kHz, and $k_\varphi = 0.003\,\mathrm{cm}^{-1}$ for $f \sim 40$ kHz, in the case of the toroidal distance 219 cm. The toroidal mode numbers estimated from these data give vanishing toroidal mode numbers $n \sim 0$. Thus, experimental data provide evidence for the symmetric spatial structure of the modes $f < 5$ kHz and $f \sim 40$ kHz supporting the conclusion on ZFs and GAM generation, respectively.

4. Conclusion

Experimental data obtained on TCABR confirm recent observations [3–7] of the amplification of long-distance

correlations in potential fluctuations during biasing L–H transitions, whereas correlations of density fluctuations are low. The LDCs are observed in the low confinement regime and increase significantly at the L–H transition.

Together with these common features, there are distinct data on the dominant frequency components in V_f for the LDCs. The LDCs are observed at frequencies $f < 20$–40 kHz without coherent modes in the TJ-II stellarator [3, 7], while it is dominated by coherent low-frequency mode $f \sim 1.6$ kHz in TEXTOR [5]. Our data are more closely related to those of TJ-II, i.e. in our experiments the LDCs are dominated by frequencies $f < 60$ kHz. We have already observed strong amplification of correlation in the L–H transition for short-distance measurements. In this case, the correlation increases for all frequencies up to a maximum measured frequency, $f_{max} = 300$ kHz in our case, and it decreases with increasing frequencies for larger distances between probes. The LDCs are accompanied by a strong decrease in the turbulent broadening of potential fluctuations in the wavenumber space.

The difference from TJ-II results is that we observed, together with the peak $f = 11$–15 kHz caused by MHD activity, two peaks in the power spectra with biasing, $f < 5$ kHz and $f \sim 40$ kHz. Both these modes show almost symmetric space structures with vanishing wave numbers, $m \sim n \sim 0$. The low-frequency fluctuations, $f < 5$ kHz, are clear indication of zonal flows [1, 2]. On TEXTOR [5] and TJ-II [3] the amplitude of the fluctuations is also enhanced at low frequencies when a bias is applied. This low-frequency potential oscillations observed during biasing have been identified as zonal flows and suggested that they could amplify and complement the fluctuation suppression linked to the mean $E \times B$ flow shear [5].

The reproducible peak at frequency $f \sim 40$ kHz with low values of wave numbers may be considered a GAM. However, taking the value of the electron temperature at the plasma edge $T_e \sim 30$ eV, measured with Langmuir probes, one expects a lower frequency, $f_{GAM} \sim 15$–20 kHz [2], in our case. At present, we do not have an explanation for this discrepancy with data from other tokamaks.

The MHD activity detected by Mirnov probes has rather strong effects on the spectra and long-distance correlations of potential fluctuations. Even a relatively low-level background MHD activity results in a peak in the power spectrum at a frequency of about 15 kHz. In spite of the electrostatic and magnetic perturbations being frequency-locked, they have quite different spatial structures. The poloidal and toroidal mode numbers of the electrostatic fluctuations caused by MHD activity show a rather large spread in the ohmic regime and low values in the bias regime.

Acknowledgments

This work was supported by FINEP (Financier of Studies and Projects), FAPESP (Supporting Agency for the Research of the State of São Paulo), IAEA (International Atomic Energy Agency) and the National Fusion Network.

References

[1] Diamond P.H., Itoh S.-I., Itoh K. and Hahm T.S. 2005 *Plasma Phys. Control. Fusion* **47** R35
[2] Fujisawa A. 2009 *Nucl. Fusion* **49** 013001
[3] Pedrosa M.A. *et al* 2008 *Phys Rev. Lett.* **100** 21503
[4] Silva C. *et al* 2008 *Phys. Plasmas* **15** 120703
[5] Xu Y. *et al* 2009 *Phys. Plasmas* **16** 110704
[6] Manz Y.P., Ramisch M. and Stroth U. 2009 *Phys. Plasmas* **16** 042309
[7] Hidalgo C. *et al* 2009 *Europhys. Lett.* **87** 55002
[8] Nascimento I.C. *et al* 2005 *Nucl. Fusion* **45** 796
[9] Nascimento I.C. *et al* 2007 *Nucl. Fusion* **47** 1570
[10] Bendat J.S. and Piersol A.G. 2010 *Random Data: Analysis and Measurements Procedures* 4th edn (New York: Wiley)
[11] Zweben S.J. *et al* 2007 *Plasma Phys. Control Fusion* **49** S1
[12] Askinazi L.G. *et al* 2006 *Plasma Phys. Control. Fusion* **48** A101
[13] Askinazi L.G. *et al* 2008 *J. Phys.: Conf. Ser.* **123** 012010
[14] Guimarães-Filho Z.O. *et al* 2008 *Phys. Plasmas* **15** 062501
[15] Scröder C. *et al* 2001 *Phys. Rev. Lett.* **86** 5711
[16] Manchandran R. *et al* 2010 *Phys. Plasmas* **17** 072515
[17] Beall J.M., Kim Y.C. and Powers E.J. 1982 *J. Appl. Phys.* **53** 3933
[18] Levinson S.J, Beall J.M., Powers E.J. and Bengtson R.D. 1984 *Nucl. Fusion* **24** 527
[19] Conway G.D. and Elliott J.A. 1987 *J. Phys. E: Sci. Instrum.* **20** 1341